Electron attachment to molecular clusters by collisional charge transfer

K. H. Bowen, G. W. Liesegang, B. S. Sanders, and D. R. Herschbach

J. Phys. Chem., **1983**, 87 (4), 557-565• DOI: 10.1021/j100227a009 • Publication Date (Web): 01 May 2002

modes whose density is reduced upon crystallite formation.

Conclusion

The above analysis of low-temperature absorption data confirms earlier reasoning that a tetracene glass formed by vapor condensation onto a cold substrate can serve as a model system for diagonal disorder. The inhomogeneous broadening of the absorption lines reflects the statistical positional disorder within the environment of an excited molecule. Observation of site splitting derived from the Davydov splitting in the crystalline counterpart structure demonstrates that off-diagonal disorder due to the variation of the exciton transfer integrals is comparatively small even in glasses formed near 4.2 K. The implication of this result is that transfer rates of electronic energy and, by analogy, also charge carriers should be described reasonably well by the product of a coupling factor characterizing electronic intersite coupling in the discrete lattice and an energy matching factor which in the case of an upward jump is simply the Boltzmann factor. This explains the success of applying recent computer simulations based on the above premises to transport phenomena in real systems.[8,21] The consistency between model predictions and experimental results also suggests that absorption measurements may be applied to predict the diffusion constant of a charge carrier in an organic single-component glass thereby making use of the common origin of the splitting of exciton and charge carrier transport bands in an amorphous organic solid.

Acknowledgment. H.B. thanks Dr. J. Klafter for a helpful discussion. Financial support by the Deutsche Forschungsgemeinschaft and the Fonds der Chemischen Industrie is gratefully achknowledged.

Registry No. Tetracene, 92-24-0.

(21) J. Lange and H. Bässler, *Phys. Status Solidi B*, in press.

Electron Attachment to Molecular Clusters by Collisional Charge Transfer

K. H. Bowen,† G. W. Liesegang,‡ R. A. Sanders,§ and D. R. Herschbach*

Department of Chemistry, Harvard University, Cambridge, Massachusetts 02138 *(Received: August 18, 1982)*

Endoergic charge transfer via $A + X_n \rightarrow A^+ + X_n^-$ in single collisions is used to study electron attachment to weakly bound molecular clusters. Two supersonic beams are employed, one to produce fast alkali atoms (usually A = Rb), the other to produce molecular clusters (typically X = Cl_2 or SO_2). From threshold energies for ion-pair formation, nominal electron affinities as a function of cluster size are derived for $(Cl_2)_n$, $Cl(Cl_2)_{n-1}$, and $(SO_2)_n$, with n = 1–4, 2–4, and 1–5, respectively. The collisional charge-transfer process which forms the negative cluster ions occurs on a subpicosecond time scale. The results are interpreted in terms of an impulsive-collision model, with incomplete vibrational relaxation for cluster ions larger than dimers.

Introduction

Solvated ions govern a host of solution phenomena, but the individual molecular species and processes often cannot be resolved or characterized in condensed phases. This has motivated the recent development of several methods for study of molecular cluster ions in the gas phase. Thermochemical data for solvation of many gaseous ions has been obtained from high-pressure mass spectrometry,[1,2] cluster ion formation in flow tubes,[3] and photoionization of molecular beams of neutral clusters.[4] Reaction rate constants[5,6] and photodestruction cross sections[7,8] have been measured for numerous ion clusters, especially for likely constituents of the D region of the ionosphere.[9] A variety of cluster ions, positive or negative, large and small, have been produced by electron bombardment of neutral clusters formed in supersonic expansions.[10-12] Theoretical studies of cluster ions have also become abundant, particularly for ion solvation by water.[13] Other pertinent work includes calculations of geometry and stability for dimer anions[14] and electron affinities as functions of cluster size for small complexes of metal atoms.[15]

This paper describes experiments designed to explore endoergic charge transfer under single-collision conditions as a method for relatively gentle electron attachment to weakly bound molecular clusters. Collisional electron transfer from alkali atoms to molecules via

$$A + B \rightarrow A^+ + B^-$$

has been extensively studied.[16] The threshold collision

† Present address: Department of Chemistry, The Johns Hopkins University, Baltimore, MD 21218.

‡ Present address: Heart, Lung, and Blood Institute, National Institute of Health, Bethesda, MD 20205.

§ Present address: Winton Hill Technical Center, Procter and Gamble Co., Cincinnati, OH 45224.

(1) Kebarle, P. "Ion-Molecule Reactions"; Franklin, J. L., Ed.; Plenum Press: New York, 1972; Vol. 1, Chapter 7 and references therein.
(2) Tang, I. N.; Lian, M. S.; Castleman, A. W. *J. Chem. Phys.* **1976**, *65*, 4022.
(3) Davidson, J. A.; Fehsenfeld, F. C.; Howard, C. J. *Int. J. Chem. Kinet.* **1977**, *9*, 17.
(4) Ceyer, S. T.; Tiedemann, P. W.; Mahan, B. H.; Lee, Y. T. *J. Chem. Phys.* **1979**, *70*, 14. Schumacher, E. *Helv. Chim. Acta* **1978**, *61*, 453.
(5) Good, A. *Chem. Rev.* **1975**, *75*, 561.
(6) Albritton, D. L. *At. Data Nucl. Data Tables* **1978**, *22*, No. 1.
(7) Cosby, P. C.; Ling, J. H.; Peterson, J. R.; Moseley, J. T. *J. Chem. Phys.* **1976**, *65*, 5267.
(8) Beyer, R. A.; Vanderhoff, J. A. *J. Chem. Phys.* **1976**, *65*, 2313.
(9) McEwan, M. J.; Phillips, L. F. "Chemistry of the Atmosphere"; Wiley: New York, 1975; and references therein.
(10) Buelow, S. J.; Worsnop, D. R.; Herschbach, D. R. *Proc. Natl. Acad. Sci. U.S.A.* **1981**, *78*, 7250.
(11) Klots, C. E.; Compton, R. N. *J. Chem. Phys.* **1978**, *69*, 1636, 1644.
(12) Gspann, J.; Körting, K. *J. Chem. Phys.* **1973**, *59*, 4726.
(13) Schuster, P.; Jakubetz, W.; Marius, W. "Molecular Models for the Solvation of Small Ions and Polar Molecules"; Springer-Verlag: West Berlin, 1975; and references therein. Kistenmacher, H.; Popkie, H.; Clementi, E. *J. Chem. Phys.* **1974**, *61*, 799.
(14) Jordan, K. D.; Wendoloski, J. J. *Chem. Phys.* **1977**, *21*, 145. Rossi, A. R.; Jordan, K. D. *J. Chem. Phys.* **1979**, *70*, 4422.
(15) Baetzold, R. C. *J. Chem. Phys.* **1971**, *55*, 4363. Cini, M. *J. Catal.* **1975**, *37*, 187. Jordan, K. D.; Simons, J. *Ibid.* **1977**, *67*, 4027. Goddard, W. *Solid State Commun.* **1978**, *28*, 501.

0022-3654/83/2087-0557$01.50/0

energy for ion-pair formation is given by

$$E_T = IP(A) - EA(B)$$

the difference in the ionization potential of the donor atom and the electron affinity of the acceptor molecule. In previous work, this electron transfer process has been used with fast alkali atom beams produced by charge exchange or sputtering to determine electron affinities for many molecules.[17] Here we adapt this method, with two essential amendments, to produce negative cluster ions and to measure the corresponding electron affinities as a function of cluster size. One amendment is use of a supersonic expansion to generate substantial concentrations of neutral molecular clusters; thus, $B = X_n$, with the range of n strongly dependent on experimental conditions. The other amendment is use of a seeded supersonic expansion to produce the fast alkali atom beam; this provides a sufficiently high atom flux to offset the relative weakness of the cluster beam.

This method for electron attachment to molecular clusters offers several advantages over electron bombardment. In the charge-transfer process, the electron jumps to the molecular cluster within the Coulombic field of the alkali cation. This obviates momentum transfer constraints. It also enables the attachment to occur isoenergetically at threshold. Fragmentation of the clusters is thereby minimized, which permits the electron affinity for an X_n cluster to be determined from the threshold energy for the X_n^- ion. In contrast, electron bombardment usually excites and dissociates the molecular cluster so the attachment is to a fragment; there is no opportunity to determine the electron affinity of the parent cluster. Another welcome feature of the charge-transfer process is its large cross section (often >100 Å^2), which makes feasible large yields of negative cluster ions.

In this study our chief aim has been to test or exemplify the anticipated properties of the charge-transfer method. We describe apparatus and experimental procedures, qualitative observations of negative ions obtained from five cluster systems, and quantitative threshold data for two systems, $(Cl_2)_n$ and $(SO_2)_n$. These two systems were selected as representative of a large class of clusters in which the electron affinity of the monomer units themselves is positive and large. Electron attachment to such clusters is expected to produce a solvated anion, $X^-(X)_{n-1}$, or ions derived from this anion. We indeed found high yields of X_n^- anions, and for the chlorine case obtained also $Cl(Cl_2)_{n-1}^-$ anions resulting from dissociative attachment. The variation of the observed thresholds and electron affinities with cluster size differs markedly for the chlorine and sulfur dioxide systems. However, a common pattern appears when the electron affinity data are interpreted in terms of an impulsive model. This suggests that the subpicosecond time scale for the electron attachment process yields incomplete vibrational relaxation for cluster ions larger than dimers.

Similar studies have been undertaken for cluster systems in which the electron affinity of the monomer units is negative. These include solvated electron systems such as water and ammonia; we hope the experiments will reveal the minimum cluster size required to capture the electron. For carbon dioxide, which belongs to this class (monomer EA ~ −0.6 eV), Quitevas[18] has recently produced cluster anions with n = 2–16; analysis of his threshold data using the impulsive model indicates that the dimer anion is quite stable (dimer EA ~ +0.9 eV).

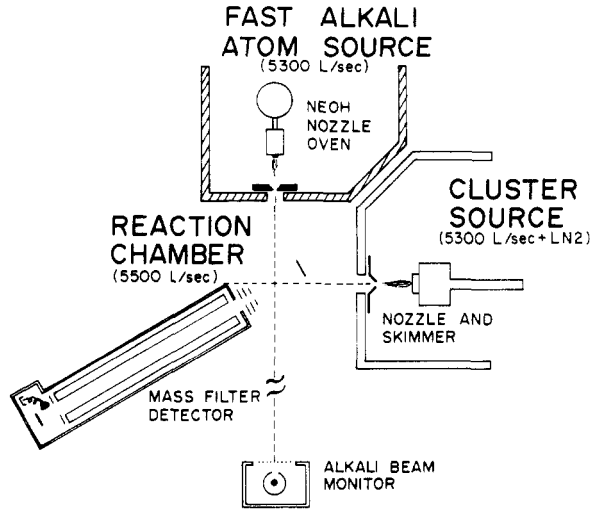

Figure 1. Schematic of the apparatus. Nominal pumping speeds in the two source chambers and the reaction chamber are indicated. Liquid-nitrogen cold traps and shields are not shown.

Apparatus and Experimental Conditions

Figure 1 shows a schematic view of the apparatus. The main features are two differentially pumped supersonic beam sources and a quadrupole mass spectrometer detector which is directed at the intersection of the two beams in the reaction chamber.

Alkali Beam Source. The fast alkali atom source has been described elsewhere.[19] It comprises a supersonic nozzle grafted onto an oven chamber. The source typically operates with an alkali partial pressure of 0.02–0.2 torr and a diluent gas pressure (usually H_2, He, Ar, or a mixture) of 800 torr. The nozzle orifice diameter is 0.15 mm. The alkali beam velocity is scanned by varying the nozzle temperature and the diluent gas. Rubidium was used in our experiments in order to take advantage of extensive velocity calibration data provided by Neoh[19] for the same nozzle and operating conditions.

The alkali atom beam obtained from this seeded supersonic source has a velocity range of about 2–5 km/s, with a velocity spread of 8% (fwhm) and a flux of 10^{16} atoms sr^{-1} s^{-1}. This flux is 10^3–10^5 larger than provided by charge-exchange or sputtering sources. The available velocity range is more limited (cf. 4–27 km/s for charge exchange, 1–15 km/s for sputtering), but this is not a handicap here because our chief interest is in the thresholds for ion-pair production.

The alkali beam intensity is monitored by an electrically shielded surface ionization detector (with a Pt–8% W alloy filament) mounted in the reaction chamber.

Cluster Beam Source. The cluster source consists of the usual supersonic nozzle and skimmer arrangement, with the separation distance externally adjustable. The nozzle is constructed from either Monel or quartz and the orifice diameter was usually 0.12 mm. A range of source conditions is employed to optimize cluster formation.[20] The main variables are as follows: (1) nozzle temperature, which can be scanned over a range of −196 to +125 °C; (2)

(16) For reviews, see: (a) Wexler, S.; Parks, E. K. *Annu. Rev. Phys. Chem.* **1979**, *30*, 1979. (b) Los, J.; Kleyn, A. W. In "The Alkali Halide Vapors"; Davidovits, P., McFadden, D. Eds.; Academic Press: New York, 1978.

(17) Hotop, H.; Lineberger, W. C. *J. Phys. Chem. Ref. Data* **1975**, *4*, 539. Janousek, B. K.; Brauman, J. I. In "Gas Phase Ion Chemistry"; Bowers, M. T., Ed.; Academic Press: New York, 1979; Vol. 2, pp 53–87.

(18) Quitevas, E. L.; Herschbach, D. R. *J. Phys. Chem.*, submitted.

(19) Larsen, R. A.; Neoh, S. K.; Herschbach, D. R. *Rev. Sci. Instrum.* **1974**, *45*, 1511.

(20) Hagena, O. F. In "Molecular Beams and Low Density Gas Dynamics"; Wegener, P. P., Ed.; Marcel Dekker: New York, 1974.

total pressure in the source, typically 1–3 atm; (3) dilution of the sample gas with argon, usually in 5- to 10-fold excess, which greatly increases the yield of clusters. For readily condensable gases such as Cl_2 and SO_2, beams containing at least 5–10% clusters are easily obtained. In a given beam, there is relatively little variation in the velocity of clusters of different size and for any size cluster the spread about the common velocity is small. These properties, typical of supersonic beams, hold because the clusters are in effect seeded either in the monomer (for a neat gas sample) or in argon (for the more typical diluted gas case).

Mass-Spectrometric Detector. The product ions are analyzed by a quadrupole mass filter. This is mounted in the reaction chamber in the plane of the crossed beams, with the axis of the quadrupole aimed at the collision zone at an angle of about 35° to the cluster beam path. The collision zone is bracketed on one side by a repeller plate and on the other by the ion extraction and lens system. An extractor plate is also located at the exit of the rod assembly. For the experiments with the Cl_2 and SO_2 systems, the product ion intensities were so large (usually $>10^{-11}$ A) that no electron multiplier was required; the cross-section measurements simply use a shielded Faraday cup. For detection of weak negative ion signals (down to about 10^{-14} A) a channeltron electron multiplier is used, with its front floated at +2 kV and its rear at about +4 kV. Signal pulses are extracted through a coupling capacitor.

The cluster formation conditions are optimized while monitoring the cluster ion signals generated by the charge-transfer process. Likewise, the mass scale is calibrated by using positive Rb^+ ions, negative monomer ions, and negative cluster ions as standards. A linear plot of mass vs. rf voltage is obtained. The maximum observable mass for this detector is 360 amu and the maximum resolution (for a large signal) is $m/\Delta m \sim 200$. The resolution is adjusted during each experimental run to maximize transmission while minimizing overlap between adjacent cluster ion mass peaks.

The mass spectrometer is not differentially pumped and thus relies on the baffled (Freon-cooled) silicone oil diffusion pumps of the reaction chamber. For typical operating conditions, the chamber pressure is $<1 \times 10^{-5}$ torr (as measured by an ionization gauge calibrated for hydrogen). Pressure measurements indicate that 90% of the gas load in the reaction chambers during experiments is due to hydrogen and/or helium from the alkali source; most of the rest is argon from the cluster source.

Figure 2 shows typical negative ion mass spectra obtained at a collision energy substantially above the thresholds for charge transfer. These spectra serve to illustrate the high signal/noise ratios in the experiments. The largest negative cluster ion peaks correspond to currents of about 10^{-9} A. For stable source conditions, the reproducibility of the negative ion mass peaks is better than ±5% over a period of several hours. However, the relative peak heights do not provide significant information. This is because the distribution of neutral cluster sizes in the parent beam and the mass dependence of the transmission of the detector are only qualitatively known and contribute opposing trends.

Procedure and Results

The experiments identify the product ions formed (via the mass spectra) and measure the dependence of relative cross sections on collision energy (scanned by varying the alkali temperature or diluent gas composition), from which the energy thresholds for production of each cluster ion are determined.

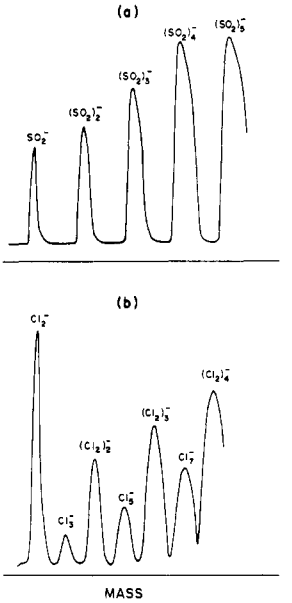

Figure 2. Typical negative ion mass spectra for (a) sulfur dioxide system and (b) chlorine system. Collision energy is 4 eV.

Ions Observed. Five cluster systems were examined: $(Cl_2)_n$, $(SO_2)_n$, $(NO_2)_n$, $SO_2(CO_2)_n$, and $(H_2S)_n$. In each case, the yield of "solvated" positive ions of the form $Rb^+(X)_n$ was much smaller (less than 1%) than the yield of negative cluster ions. Very large signals from "bare" Rb^+ ions (typically $>10^{-8}$ A) were observed, but extensive signal averaging was required to detect any other positive ion species (for which typical signals are $\simeq 10^{-13}$ A). Thus, here we present only observations of negative ions.

As seen in Figure 2, the chlorine cluster system yields negative ions corresponding to electron attachment with and without breaking chemical bonds. The latter ions, $(Cl_2)_n^-$, were detected for n = 1–4; still larger cluster ions could probably be observed easily with a mass spectrometer of sufficient range. The ions produced by dissociative attachment, of the form $Cl^-(Cl_2)_{n-1}$, were detected for n = 2–4. These correspond to the well-known polyhalide ions;[21] as noted below, the threshold for dissociative attachment involves the bond strength of Cl_2 and the electron affinity of the polyhalide radical. For the sulfur dioxide cluster system, $(SO_2)_n^-$ ions with n = 1–5 were detected; only negligibly weak signals were observed for ions resulting from attachment with disruption of chemical bonds. The range of collision energy extended up to 6 eV.

The nitrogen dioxide system is another example for which the monomeric molecule has a large, positive electron affinity. With the Faraday cup detector, we found that the only negative ion observable for beams of neat NO_2 was the NO_2^- ion. A strong negative cluster ion spectrum appeared for beams of NO_2 seeded in argon. However, only odd-numbered $(NO_2)_n^-$ cluster ions with n = 1, 3, 5, ... were seen.[22] Since ordinary positive ion mass spectra yield $(NO_2)_n^+$ with predominantly odd-n ions (although even-n ions also appear), it seems likely that odd-n neutral clusters are more abundant than even-n clusters for nitrogen dioxide.[23]

Large yields of the mixed cluster ions $(SO_2)^-(CO_2)_n$, with n = 1–5, were observed when carbon dioxide was admitted to a gas line that had previously contained sulfur dioxide,

(21) Tasker, P. W. *Mol. Phys.* **1977**, *33*, 511 and references cited therein.

(22) Bowen, K. H.; Liesegang, G. W.; Herschbach, D. R. *Faraday Discuss. Chem. Soc.* **1979**, *67*, 145.

(23) Novick, S. E.; Howard, B. J.; Klemperer, W. *J. Chem. Phys.* **1972**, *57*, 5619.

even after pumping on the line for about 1 h beforehand. Since CO_2 has a negative electron affinity, these ions correspond to solvation of SO_2^-. This system illustrates how sensitive the clustering process can be to contaminants. The neutral $SO_2(CO_2)_n$ species and other mixed clusters have been previously observed in the gas phase.[24]

For hydrogen sulfide, the monomeric molecule has a large negative electron affinity. Thus, if electron attachment to a cluster occurs without dissociation of chemical bonds, the cluster anion corresponds to a gas-phase solvated electron. The hydrogen sulfide system appeared promising because it yielded weak negative ion mass peaks starting at about the $n = 4$ region (or perhaps $n = 3$) and extending up to $n = 9$, the limit of our mass range. On examining this spectrum under high resolution, however, we found that the observed ions correspond to dissociative attachment with multiple loss of hydrogen atoms; no intact $(H_2S)_n^-$ cluster anions appear in the accessible mass range.

Cross Sections and Thresholds. The primary data for our relative cross-section measurements consists of corresponding sets of negative ion mass spectra, alkali beam intensities, and alkali nozzle temperatures. We first outline the data reduction procedure assuming that all velocities are sharply defined and the signal S_i for a given cluster ion species arises solely from the corresponding neutral parent cluster. Then, aside from a normalization factor, S_i is given by

$$S_i = \sigma_i v_R n_A n_B \quad (1)$$

where σ_i is the cross section for $A + B \rightarrow A^+ +$ species i (either B^- or a fragment ion if dissociative attachment occurs); v_R is the relative velocity of the colliding beams; n_A and n_B are the number densities of the alkali beam and the appropriate neutral cluster component in the collision zone. For the alkali beam, n_A is determined from the ratio of the beam flux density I_A monitored by the surface ionization detector and the beam velocity v_A obtained from the nozzle temperature and calibration measurements for the various diluent gases used.[19] For the cluster component, n_B is not determined but is held constant during a given experiment by maintaining the cluster beam source conditions. The relative cross section is thus given by

$$\sigma_i = (S_i/I_A)(v_A/v_R) \quad (2)$$

Since the reactant beams intersect at 90°, the relative velocity is obtained from $v_R = (v_A^2 + v_B^2)^{1/2}$. The corresponding relative kinetic energy is given by $E_R = {}^1/_2\mu_{AB}v_R^2$, with the reduced mass $\mu_{AB} = m_A m_B/(m_A + m_B)$.

Figures 3–5 present the relative cross-section functions $\sigma_i(E_R)$ evaluated in this way. For the sulfur dioxide system, four carrier gases (pure H_2 or He, and two mixtures) were used as diluents for the seeded alkali beams, in order to extend the measurements over a wider range of collision energy. The data segments taken with different diluent gases did not always overlap perfectly, probably due to long-term variation in n_B. These segments were normalized by using points at the same E_R values; however, this was done only for segments that overlapped in regions with the cross section essentially a linear function of collision energy. For the chlorine system, the thresholds occur at lower E_R and thus all the data were taken with pure He as the diluent. The cross sections for cluster anions formed without disruption of chemical bonds (Figure 4) are plotted separately from those for dissociative attachment (Figure 5). Data for production of the atomic anion Cl^- were not obtained, since our energy range extends barely above the threshold (3.1 eV) for this species.

(24) Calo, J. M. *Nature (London)* **1974**, *248*, 665.

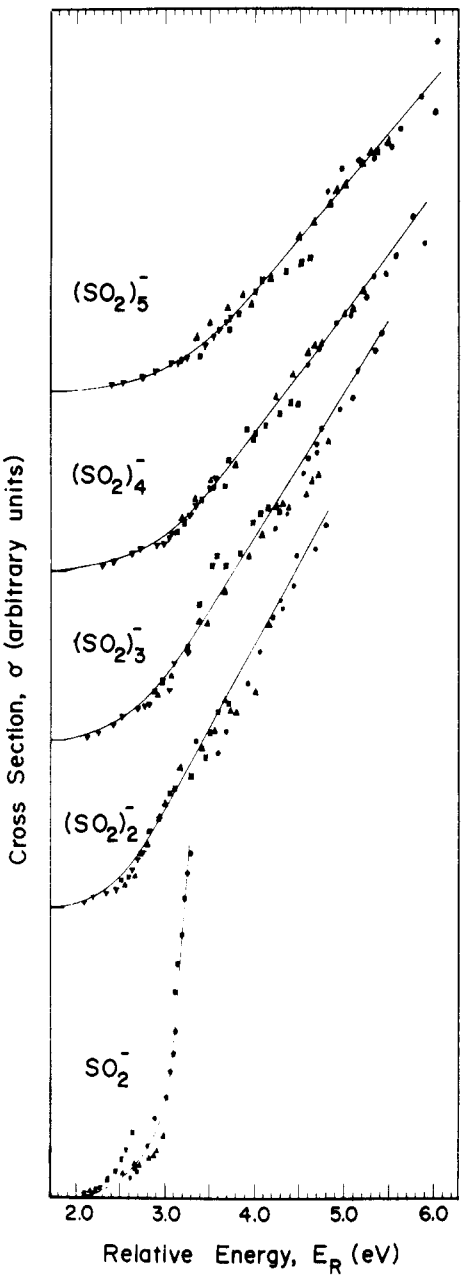

Figure 3. Energy dependence of cross sections for endoergic charge transfer to produce cluster anions, for the $(SO_2)_n$ system with $n = 1$–5. In the seeded supersonic alkali atom beam four diluent gases were used: pure H_2 (●), 72.7% H_2/27.3% He (▲), 58% H_2/42% He (□), and pure He (▼). Ordinate scale is the same for the various cluster ions but the origin for each species is shifted upward to avoid overlapping of data.

The chief features of the cross sections are as follows: (1) In each case, the energy dependence is practically linear over our range, aside from the "tails" near threshold. (2) The slopes of the linear portions tend to decrease as the size of the cluster anion increases, although for sulfur dioxide this decrease occurs mostly as monomer → dimer. (3) The location of the thresholds shows only a modest variation with cluster size for each system, except again there is a substantial change for sulfur dioxide as monomer → dimer. Table I lists values of the threshold energies E_T obtained by extrapolating the linear portions of the cross sections and corresponding relative values for the slopes, $d\sigma_i/dE_R$. Also included are nominal electron affinities EA derived and discussed below.

Before examining the trends found in the cross-section parameters, we discuss experimental limitations neglected in the data reduction. The main sources of error are im-

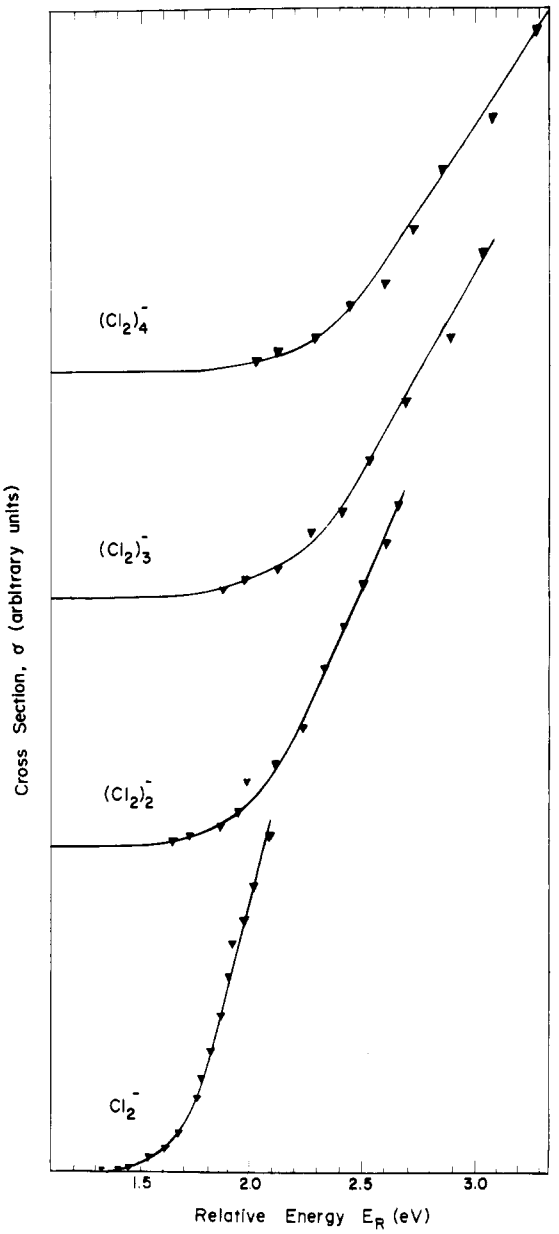

Figure 4. Energy dependence of cross sections for production of cluster anions, for the $(Cl_2)_n$ system with n = 1–4.

TABLE I: Cross-Section Parameters

anion	E_T, eV	EA, eV	$d\sigma_i/dE_R$
Cl_2^-	1.7	2.5	(1.00)
$(Cl_2)_2^-$	2.0	2.2	0.56
$(Cl_2)_3^-$	2.2	2.0	0.47
$(Cl_2)_4^-$	2.3	1.9	0.39
Cl_3^-	2.1	4.6	(1.00)
Cl_5^-	2.3	4.4	0.67
Cl_7^-	2.4	4.2	0.54
SO_2^-	3.0	1.2	(1.00)
$(SO_2)_2^-$	2.3	1.9	0.12
$(SO_2)_3^-$	2.6	1.6	0.11
$(SO_2)_4^-$	2.8	1.4	0.08
$(SO_2)_5^-$	3.1	1.1	0.08

perfect velocity definition, fragmentation of clusters, and drifts in source and detector conditions. Thermal spreads in the parent beam velocities account for the tails near threshold.[25] As in comparable experiments,[26] linear extrapolation ignoring the tails appears satisfactory, since the thresholds that we find for the Cl_2 and SO_2 monomer molecules agree with the electron affinities determined in previous work.[17] Also to be considered is velocity slip[27] in the cluster beam, which increases with cluster size. From calculations employing extreme values of v_B, we found that the effect is negligible in our data reduction. The results are insensitive because $v_R \simeq v_A \gg v_B$. Thus, we used values for v_B from time-of-flight measurements for similar beam sources in this laboratory. For instance, such measurements (at 25 °C) gave average velocities of 450 and 410 m/s for the chlorine monomer and dimer, respectively.[28]

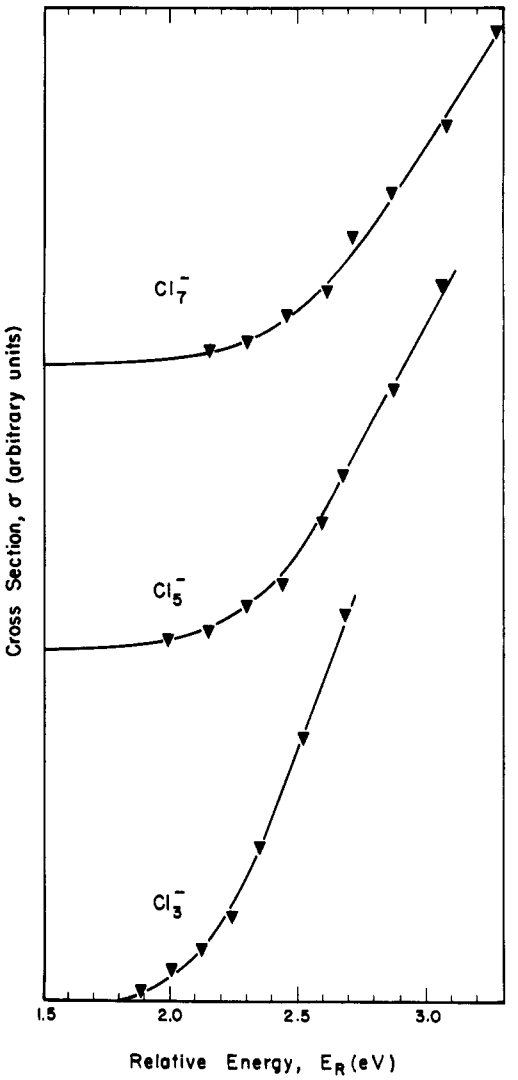

Figure 5. Energy dependence of cross sections for production of cluster anions, for the $Cl(Cl_2)_{n-1}$ system with n = 2–4.

If extensive fragmentation occurs for cluster bonds (rather than chemical bonds), the fragments from large clusters will distort the cross sections and energy scale derived for the smaller clusters. Such fragmentation might also contribute to the tails. As a test, we measured the relative cross section for production of SO_2^- for a wide range of source conditions, including mild conditions under which the yield of cluster ions became unobservably small. The cross-section threshold and slope remained the same, and also the tail region. This is a reasonable test unless fragmentation of clusters fails to produce any monomer

(25) Chantry, P. J. *J. Chem. Phys.* **1971**, *55*, 2746.
(26) Mathur, B. P.; Rothe, E. W.; Tang, S. Y.; Reck, G. P. *J. Chem. Phys.* **1976**, *65*, 565.
(27) Anderson, J. B. *Entropie* **1967**, *18*, 33.
(28) Dixon, D. A.; Herschbach, D. R. *Ber. Bensenges. Phys. Chem.* **1977**, *81*, 145.

TABLE II: Parameters Pertinent to Ion-Pair Formation[a]

quantity	value, eV	ref
IP(Rb)	4.18 ± 0.0001	29
D(Cl-Cl)	2.48 ± 0.004	30
D(O-SO)	5.66 ± 0.09	30
EA(Cl)	3.615 ± 0.004	17
$EA^a(Cl_2)$	2.45 ± 0.15	17
$EA^v(Cl_2)$	1.3 ± 0.5	31
EA(O)	1.462 ± 0.003	17
$EA^a(SO)$	1.09 ± 0.01	17
$EA^a(SO_2)$	1.10 ± 0.04	17

[a] Superscripts a and v denote adiabatic and vertical, respectively.

ions; that seems unlikely, certainly for the dimer clusters. Likewise, the good reproducibility found for cross-section measurements made with substantially different cluster beam conditions offers evidence that cluster fragmentation is not a significant problem in this experiment.

From comparison of our monomer cross sections with previous results and from the scatter of our data, we estimate the precision to be ±0.15 eV for our threshold values and about 10% for the cross-section slopes.

Kinematic Aspects

To assess the trends seen in the threshold data of Table I, we examine first some consequences of energy conservation. For direct ion-pair formation via $A + X_n \rightarrow A^+ + X_n^-$, a nominal electron affinity for the parent neutral cluster is defined by

$$EA(X_n) = IP(A) - E_T \quad (3)$$

the difference between the ionization potential of the alkali atom and the minimum relative kinetic energy required to reach the threshold. This nominal affinity is related to the adiabatic electron affinity of a monomer unit by

$$EA(X_n) = EA(X) - CD(X\cdots X_{n-1}) + CS(X^-\cdots X_{n-1}) - CE(X_n^-) \quad (4)$$

Here CD is the dissociation energy for detaching a neutral monomer from the neutral cluster; CS is the total solvation energy for a monomer anion interacting with all the other neutral monomer units (including any exoergicity released by chemical rearrangement of the cluster); and CE denotes any internal excitation of the cluster anion produced by the electron attachment process. If dissociative attachment occurs (for $X = Y_2$), in effect $X_n^- \rightarrow Y^-X_{n-1} + Y$. The nominal electron affinity in eq 3 is then replaced by

$$EA(YX_{n-1}) = EA(Y) - D(Y_2) - CD(X\cdots X_{n-1}) + CS(Y^-\cdots X_{n-1}) - CE(Y^-X_{n-1}) \quad (5)$$

where D is the bond dissociation energy of the monomer molecule ($X = Y_2$) that accepts the electron. These formulas relating the nominal electron affinity to EA(X) or EA(Y) assume that the threshold energy E_T does not include any activation energy for electron transfer and at threshold the relative translational energy of the products is also negligibly small. For the many systems examined in previous studies of ion-pair formation in collisions of alkali atoms with monomer molecules,[16] these properties appear to hold.

Table II lists the parameters[29-31] required to predict the threshold energies for the monomer case ($n = 1$). The thresholds that we find for electron transfer to Cl_2 and SO_2 without dissociation, 2.5 and 1.2 eV, respectively, agree well with well-established values for the adiabatic electron affinities.[17] For dissociative attachment to the monomer molecules, eq 5 predicts that the thresholds for appearance of Cl^-, O^-, and SO^- are 3.1, 8.4, and 8.9 eV, respectively. Our observation of dissociative attachment for chlorine but not for sulfur dioxide is consistent with these numbers.

TABLE III: Estimated Adiabatic Electron Affinities (in eV)

Y^- [a]	$EA^a(Y)$	X	$\Delta(EA)$[b]	ref
O_2^-	0.43	H_2O	0.8, 0.7, 0.7, 0.6, 0.5	32
NO_3^-	3.9	H_2O	0.5, 0.5	33
		HNO_3	1.2, 0.8, 0.7	3

[a] Parent ion. [b] $n = 1, \ldots$. Here $\Delta(EA) = EA^a(YX_n) - EA^a(YX_{n-1})$ is the increment in the adiabatic electron affinity for addition of successive solvent molecules, X = H_2O or HNO_3.

For the cluster systems, only limiting estimates of the thresholds can be made. For adiabatic interactions, the internal excitation CE = 0. The monomer detachment energy CD and the solvation energy CS (in eV units) are expected to be roughly given by CD $\sim 0.05(n-1)$ and CS $\sim 0.5(n-1)$ for small clusters, in accord with typical van der Waals and ion–solvent interaction energies. These quantities should become independent of n for sufficiently large clusters for which the mean number of neighbors becomes constant. Thus, for small clusters the adiabatic electron affinity is expected to increase monotonically with cluster size, by roughly 0.5 eV for each added monomer unit. Other experiments that explicitly measure electron affinities as a function of cluster size are not available at present, but in a few cases adiabatic electron affinities for cluster species can be estimated from thermochemical data. Table III gives results for three such systems.[32,33] In each case the expected monotonically increasing trend appears, and the increment per solvent molecule is indeed typically $\Delta(EA) \sim 0.5$–0.8 eV.

The nominal electron affinities that we find in Table I behave quite differently. For the $(Cl_2)_n$ system, the nominal EA decreases gradually with cluster size, by about 0.2 eV per Cl_2 unit. For the $(SO_2)_n$ case, the EA increases by 0.7 eV for monomer → dimer but thereafter decreases by about 0.3 eV per SO_2 unit. For the $Cl(Cl_2)_{n-1}$ system resulting from dissociative attachment, the EA likewise has a nonmonotonic variation if the value for the chlorine atom ($n = 1$) is included; thus, the EA increases by 1.0 eV for $Cl \rightarrow Cl_3$ and thereafter decreases by about 0.2 eV per Cl_2 unit. These trends indicate that our nominal EA's are not adiabatic electron affinities, except for the monomer species and possibly for the sulfur dioxide dimer and the chlorine atom trimer. The larger cluster anions appear to be formed with substantial internal excitation. A dynamical model thus is required to interpret the threshold energies for these systems.

Impulsive Model

Since the neutral clusters are held together only by weak van der Waals forces, they must have loose, "floppy" structures in which the monomer units retain essentially the properties of isolated molecules. The initial electron transfer therefore seems likely to involve a single monomer unit. The threshold behavior and the degree to which the corresponding nominal electron affinity approaches the

(29) Moore, C. E. "Atomic Energy Levels"; National Bureau of Standards: Washington, DC, 1970; *Natl. Stand. Ref. Data Ser.* (*U.S., Natl. Bur. Stand.*), No. 35.
(30) Darwent, B. deB. "Bond Dissociation Energies in Simple Molecules"; National Bureau of Standards: Washington, D.C, 1970; *Natl. Stand. Ref. Data Ser.* (*U.S., Natl. Bur. Stand.*), No. 31.
(31) Person, W. B. *J. Chem. Phys.* **1961**, *38*, 109.
(32) Tabulated in: Phelps, A. V. "Defense Nuclear Agency Reaction Rate Handbook", DNA 1948-H, 2nd ed.; Bortner, M. H., Baurer, T.; Eds.; 1972.
(33) Fehsenfeld, F. C.; Ferguson, E. E. *J. Chem. Phys.* **1974**, *61*, 3181.

adiabatic value then depend on the extent to which the monomer accepting the electron interacts with other monomer units during the brief time that the alkali atom donor interacts with the cluster.

In deriving the nominal electron affinities given in Table I, we have as usual computed the threshold energies from the relative kinetic energy $E(A–X_n)$ of the alkali atom and the full cluster. This tacitly assumes a long interaction time that permits all the monomer units in the cluster to participate in the electron attachment process. We shall refer to that limiting case as the "full-cluster model". If the interaction is so brief that only a single monomer unit participates, we need to recompute the threshold energies using the relative kinetic energy $E(A–X)$ of the alkali atom with respect to just the monomer unit.[34] This limiting case corresponds to a completely impulsive collision and we refer to it as the "monomer-impulsive model". From an estimate of the collision duration and from further analysis of our threshold data, we find evidence that for dimers and larger clusters the electron attachment indeed can be described by the impulsive model.

Collision Duration. As exemplified in much previous work,[16] the alkali valence electron "harpoons" the target molecule when the incident atom reaches a radius R_c defined by crossing of covalent and ionic potential surfaces. Since the electron jump is a nonadiabatic Franck–Condon process,[35] the newly formed negative molecule–ion may contain vibrotational excitation. In the course of the collision this excitation may be entirely or partly relaxed, however, due to perturbations induced by the very strong transient Coulombic field of the departing alkali cation.[36] The relaxation is in fact complete for many small, chemically bound molecules studied previously, as shown by agreement between the observed threshold energies and adiabatic electron affinities determined by other means.[17]

The collision duration during which the alkali cation is available to relax the molecular anion can be estimated from the crossing radius and relative velocity as $\Delta t \simeq 2R_c/v_R$, with $R_c \simeq e^2/(IP - EA^v)$ determined by the difference between the ionization potential of the alkali and the vertical electron affinity of the target molecule. Using a typical velocity at threshold, $v_R \sim 3000$ m/s, and monomer values for EA^v, we find for both the Cl_2 and SO_2 systems that $\Delta t \sim 3 \times 10^{-13}$ s. This time is comparable to the vibrational period of a "soft" chemical bond. In view of the results for small target molecules,[16] such a Δt is probably adequate for complete relaxation of the monomer unit that receives the electron. For cluster molecules relaxation may be far less facile. Monomer units well removed from the initial attachment site will usually need to reorient or rearrange to achieve optimum solvation of the added charge and thereby produce a cluster configuration corresponding to the adiabatic electron affinity.

This process is probably comparable to molecular reorientation in a condensed phase. Nice evidence for an analogous process in solution is provided by a correlation of rates of electron solvation by alcohols with rotational relaxation times.[37] Clusters produced in a supersonic expansion are expected to resemble a condensed phase by virtue of their low internal temperatures, and this is confirmed by fluorescence spectra.[38] Typical rotational relaxation times[39] vary from 10^{-11}–10^{-10} s in some polar liquids to 10^{-6} s in viscous liquids to 10^{-2}–10^{2} s in molecular solids. Only relaxation that occurs during the collision can affect the observed threshold energies. Thus, we conclude that, except for quite small clusters, a subpicosecond collision duration is much too short to permit adiabatic electron attachment.

TABLE IV: Impulsive-Model Analysis

anion	electron affinities, eV $k = 1$	electron affinities, eV $k = 2$	nonadiabatic ΔE, eV $k = 1$	nonadiabatic ΔE, eV $k = 2$
Cl_2^-	2.5			
$(Cl_2)_2^-$	2.8	2.2	0.6	
$(Cl_2)_3^-$	2.8	2.3	0.8	0.3
$(Cl_2)_4^-$	2.8	2.3	0.9	0.4
Cl^-	3.6			
Cl_3^-	5.1	4.6	0.5	
Cl_5^-	5.2	4.7	0.8	0.3
Cl_7^-	5.2	4.7	1.0	0.5
SO_2^-	1.2			
$(SO_2)_2^-$	2.5	1.9	0.6	
$(SO_2)_3^-$	2.6	2.0	1.0	0.4
$(SO_2)_4^-$	2.6	1.9	1.2	0.5
$(SO_2)_5^-$	2.5	1.9	1.4	0.8

Active Subcluster. The simplest impulsive model assumes an adiabatic electron transfer to a subcluster of only k monomer units

$$A + X_k \cdots X_{n-k} \rightarrow A^+ + X_k^- \cdots X_{n-k}$$

The rest of the cluster, X_{n-k}, merely acts as a spectator. The relative kinetic energy of the alkali atom with respect to the active subcluster X_k is related to that with respect to the whole cluster by

$$E(A–X_k) = f_k E(A–X_n) \quad (6)$$

where f_k is the ratio of the reduced mass for A,X_k to that for A,X_n. It is given by

$$f_k = 1 - [(n - k)/n][m_A/(m_A + km_X)] \quad (7)$$

Table IV lists electron affinities derived from the observed threshold energies using this impulsive model. The analysis involves simply replacing the term $E_T(A–X_n)$ in eq 3 with the corresponding $E_T(A–X_k)$ from eq 6. The same treatment applies for dissociative attachment, since the kinetic energy enters in the same way, regardless of the subsequent breakup of the initially formed X_n^- anion. Results are given for $k = 1$, the monomer-impulsive model, and for $k = 2$, the dimer-impulsive model. Figure 6 provides a comparison with the case $k = n$ (used in Table I), the full-cluster model.

Ideally, for a given system, the impulsive model (with a suitable choice of k) would yield the same EA value for all cluster sizes (with $n \geq k$). The monomer-impulsive model indeed gives constant EA values (within experimental scatter) for each of the three systems studied, for dimer and larger clusters ($n \geq 2$). However, in each case this constant EA is substantially larger than the monomer electron affinity. The jump in EA between $n = 1$ and $n \geq 2$ might be attributed to solvation of the initially formed monomer anion X^- by its nearest neighbor in the cluster. Despite the subpicosecond collision duration, polarization forces from charge-induced dipoles can take part. The nearest neighbor molecule probably need not adjust its situation within the cluster in order to exert practically

(34) Mahan, B. H. *J. Chem. Phys.* **1970**, *52*, 5221.
(35) Anderson, R. W.; Herschbach, D. R. *J. Chem. Phys.* **1975**, *62*, 2666.
(36) Havemann, U.; Zülicke, L.; Nikitin, E. E.; Zenbekov, A. A. *Chem. Phys. Lett.* **1974**, *25*, 487.
(37) Kenney-Wallace, G. A. *Acc. Chem. Res.* **1978**, *11*, 433.
(38) Saenger, K. L.; McClelland, G. M.; Herschbach, D. R. *J. Phys. Chem.* **1981**, *85*, 3333.
(39) Pimentel, G. C.; McClellan, A. L. "The Hydrogen Bond"; W. H. Freeman: San Francisco, 1960.

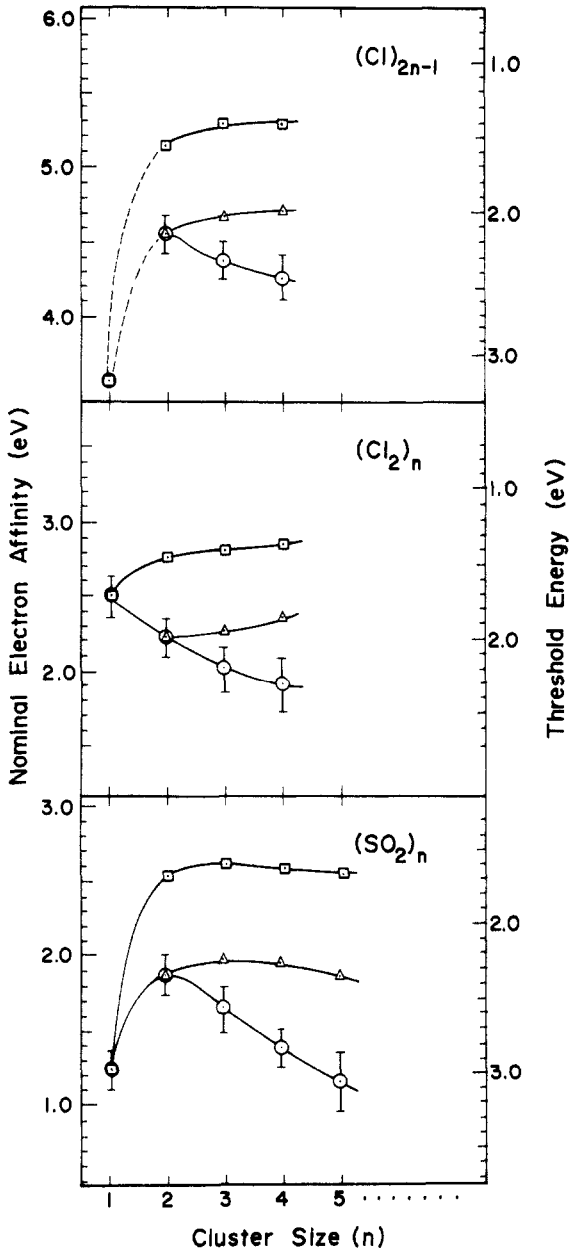

Figure 6. Threshold energies and nominal electron affinities as functions of cluster size, for chlorine atom, chlorine molecule, and sulfur dioxide systems. Results are shown for three models employed in data analysis: full-cluster model (O); monomer-impulsive model (□); and dimer-impulsive model (△). Error bars shown for the full-cluster results also apply for the other two models.

the full solvation effect. The apparent onset of impulsive character at $n = 2$ led us to try the dimer-impulsive model. It again gives constant EA values (for $n \geq 2$). For each system, the magnitude of the constant EA is lower than that for the monomer-impulsive model by ~0.5–0.6 eV. A dubious result is the EA for $(Cl_2)_2$, which the dimer-impulsive model finds to the *lower* (~2.2 eV) than for Cl_2 (2.5 eV), rather than *higher* as expected due to the solvation contribution. This suggests that electron attachment to the chlorine dimer is not fully adiabatic. In either its monomer or dimer variants, however, the impulsive model clearly proves much more satisfactory than the full-cluster model in interpreting the threshold data.

Since the impulsive model implies that electron attachment is nonadiabatic for clusters with $n > k$, the corresponding vibrotational excitation $\Delta E(n,k)$ of the cluster anions can be derived from the model. This is given by

$$\Delta E(n,k) = E_T(A\text{–}X_n) - E_T(A\text{–}X_k) \quad (8)$$

$$= (1 - f_k)E_T(A\text{–}X_n) \quad (9)$$

$$= EA(X_k) - EA(X_n) \quad (10)$$

In the last line, the first term refers to the electron affinity from the impulsive model (given in Table IV) and the second term to that from the full-cluster model (in Table I). Values of ΔE are included in Table IV. As noted, the observed jump between $n = 1$ and $n \geq 2$ in EA from the monomer-impulsive model might be due to dimeric solvation. If so, this also enters into the nominal ΔE. Thus, the part of ΔE attributable to internal excitation would be about the same as that from the dimer-impulsive model. In any case, these estimates indicate that the larger cluster anions contain substantial excitation.

Thermochemical Aspects

Some of the evidence for impulsive attachment derived from our threshold data can be sharpened by thermochemical considerations. The adiabatic electron affinities and bond dissociation energies of clusters that differ by addition of one monomer unit are related by

$$EA(X) + D(X^-\text{–}X_n) = EA(X_n) + D(X\text{–}X_n^-) = EA(X_{n+1}) + D(X\text{–}X_n) \quad (11)$$

These identities are readily obtained by constructing cycles between the components $X_n + X + e^-$ and the X_{n+1}^- cluster anion. Removal of X^- or X from the X_{n+1}^- cluster anion should require more energy than removal of X from the X_{n+1} neutral cluster, since solvation energies exceed van der Waals bond strengths. Consequently, $EA(X_{n+1})$ should be larger than either $EA(X_n)$ or EA(X). Iteration with $n = 2, 3, \ldots$ then requires the adiabatic electron affinity to increase monotonically with cluster size. This criterion confirms our heuristic conclusion that the full-cluster model is incompatible with our data.

The same thermodynamic identities offer further tests of the monomer and dimer versions of the impulsive model. For the $n = 1$ case

$$EA(X) + D(X_2^-) = EA(X_2) + D(X_2) \quad (12)$$

where the van der Waals bond strength $D(X_2)$ is negligibly small. For $X = Cl_2$, we find (from Tables I and IV) that the monomer model yields a reasonable solvation energy, $D(X_2^-) = 0.3$ eV, but the dimer gives an unacceptable negative value, $D(X_2^-) = -0.3$ eV. However, for $X = SO_2$, the corresponding monomer and dimer results are $D(X_2^-) = 1.4$ and 0.8 eV. A recent experimental measurement of this solvation energy gives 1.0 eV, a result between our two models.[40]

Another comparison is available for the Cl_3^- formed by dissociative attachment. An adiabatic value of $EA(Cl_3) = 5.14$ eV has been estimated recently from thermochemical data.[41] This agrees well with the value 5.1 eV obtained from the monomer model, less well with the 4.6 eV from the dimer model.

Discussion

Our impulsive-model analysis suggests that the dimer has a special status. As noted, this might result from the readiness of a nearest neighbor to "switch on" its solvation interaction with the monomer anion created on arrival of the electron. Here we consider further this and two other possible explanations for the onset of impulsive behavior

(40) Keesee, R. G.; Lee, N.; Castleman, A. W. *J. Chem. Phys.* **1980**, *73*, 2195.

(41) Lee, L. C.; Smith, G. P.; Moseley, J. T.; Cosby, P. C.; Guest, J. A. *J. Chem. Phys.* **1979**, *70*, 3237; *71*, 4770.

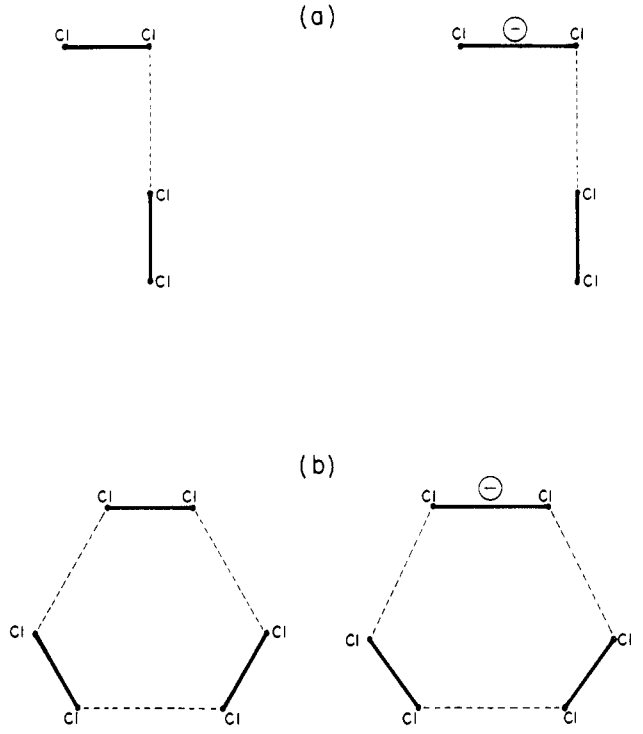

Figure 7. Schematic illustration of structural changes that might accompany attachment of an electron to (a) a chlorine dimer or (b) a chlorine trimer.

with the dimer rather than the monomer. These various interpretations raise questions that can only be resolved by structural data.

For clusters of molecules with large electron affinities, such as Cl_2 and SO_2, it appears plausible that the added electron resides on a single molecule. For $Cl_2 \rightarrow Cl_2^-$, the bond lengthens appreciably, whereas $SO_2 \rightarrow SO_2^-$ produces no significant changes in geometry.[42] Electric deflection experiments indicate that $(Cl_2)_2$ and $(SO_2)_2$ are polar and thus have open structures while $(Cl_2)_3$ and $(SO_2)_3$ are nonpolar and presumably form closed symmetric rings.[43] For $(Cl_2)_2$ there is evidence for an "L-shaped" structure with three of the chlorine atoms almost collinear.[44] Figure 7 pictures the expected configurations of the chlorine neutral dimer and trimer and the similar but entirely hypothetical configurations of the negative ions. The solvation contribution to the threshold energy corresponds to a subpicosecond "snapshot" of the negative ion structure. The observed constancy of EA obtained from the monomer-impulsive model (Table IV) is now seen to have a curious implication. The solvation contribution of 0.3 eV is the same for the dimer, trimer, and tetramer. Yet for the dimer this 0.3 eV is attributed to nearly optimal placement of a single solvent molecule, whereas for the trimer or tetramer it is attributed to nonoptimal placement of a pair or trio of solvent molecules. Such a situation is possible but seems dubious.

Another rationalization for the jump in EA as monomer → dimer is a very rapid internal ion–molecule reaction within the dimer to form a more stable isomeric anion. Plausible candidates would be $Cl_3^-\cdots Cl$ and $SO_3^-\cdots SO$. The former is slightly more stable than $Cl_2^-\cdots Cl_2$, but the latter can be ruled out, since $SO_2^-\cdots SO_2$ is more stable by >1 eV (from Table II). Also, since the Cl_3^- moiety has a collinear, nearly symmetric structure,[21] it could form within the L-shaped dimer by merely extending one of the Cl_2 bonds (along the dashed line in Figure 7a) during the electron attachment. The bond extension known to occur for the monomer case[42] within the collision duration has the required magnitude, about 0.5 Å. Yet formation of $Cl_3^-\cdots Cl$ (and analogous isomeric anions for larger clusters) in time to affect the threshold energy appears not to occur; otherwise the observed EA should be much higher, near 5 eV.

Resonant charge transfer of the electron among the monomer units is another quick-acting process which could increase EA for the dimer and larger clusters. This would be inhibited by the bond extension that occurs in the Cl_2^- case, but not for the SO_2^- case. Extra stabilization by charge sharing thus might account for the much larger monomer → dimer jump in EA observed for the sulfur dioxide system. Again, however, it is unclear why such stabilization would not continue to increase for larger clusters.

As illustrated in these experiments and elsehwere,[45] endoergic electron transfer from fast alkali atoms offers a relatively gentle way to produce large yields of negative ions of fragile molecular complexes. The method also enables measurements of threshold energies but suffers from a major limitation imposed by the subpicosecond collision duration. Our results indicate that this does not permit adiabatic electron attachment to clusters larger than dimers.

However, the method still has a useful role, in the present exploratory era. If the monomer units have positive electron affinities, the adiabatic electron affinities of clusters can be estimated from solvation energy measurements and other thermochemical data (as in Table III and the Cl_3 case[41]). As yet such information has been obtained for only a few systems, and thus our results for $(Cl_2)_2$ and $(SO_2)_2$ are the only reported values for these dimers.[46] The thermochemical route cannot be used for clusters in which the monomer units have negative electron affinities, the "solvated-electron" regime. Again, electron transfer from alkali atoms to $(CO_2)_2$ has recently provided the only available experimental EA value for a system in this regime.[18] More incisive studies of clusters must apply detection techniques such as photodetachment spectroscopy to obtain structural parameters as well as better electron affinities.

Acknowledgment. We thank William Klemperer, Yuan Lee, and Peter Wolynes for useful suggestions; Doug Worsnop, Ed Quitevis, and Florence Lin for help with some of the measurements; Rich Cavanagh and Bob Altman for examining the polarity of the sulfur dioxide dimer and trimer; and George Pisiello and the machine shop for exceptional craftsmanship and zeal in construction of the apparatus. We are grateful for support of this research by the National Science Foundation.

Registry No. Rb, 7440-17-7; Cl_2, 7782-50-5; SO_2, 7446-09-5.

(42) Massey, H. "Negative Ions", 3rd ed.; Cambridge University Press: London, 1976.

(43) For chlorine: Harris, S. J.; Novick, S. E.; Winn, J. S.; Klemperer, W. *J. Chem. Phys.* **1974**, *61*, 3866. For sulfur dioxide R. R. Cavanagh and R. S. Altman, private communication.

(44) Prissette, J.; Kochanski, E. *J. Am. Chem. Soc.* **1978**, *100*, 6609.

(45) Yokozeki, A.; Quitevas, E. L.; Herschbach, D. R. *J. Phys. Chem.* **1982**, *86*, 617.

(46) For $(SO_2)_2$ an EA ~ 2 eV can be roughly estimated from data given in ref 40. In this calculation, the dissociation energy of X_2^- is approximated by the enthalpy change for $X^- + X \rightarrow X_2^-$ and the bond dissociation energy of X_2 is presumed negligibly small (where $X = SO_2$). For larger clusters, the propagation of errors by iteration of thermochemical cycles becomes prohibitive.